The evaluation of the effective thermal conductivity of metal-foam loaded phase change materials

Claudia Naldi, Matteo Dongellini, Gian Luca Morini

The evaluation of the effective thermal conductivity of metal-foam loaded phase change materials

In: Journal of Energy Storage, Volume 51, 2022, 104450

https://doi.org/10.1016/j.est.2022.104450

The evaluation of the effective thermal conductivity of metal-foam loaded phase change materials

Claudia Naldi*, Matteo Dongellini, Gian Luca Morini

Department of Industrial Engineering

Alma Mater Studiorum – University of Bologna

Viale del Risorgimento 2, 40136, Bologna, Italy

*Corresponding author:

Dr. Claudia Naldi

E-mail: claudia.naldi2@unibo.it

Other e-mails: matteo.dongellini@unibo.it; gianluca.morini3@unibo.it

Abstract

Phase Change Materials (PCMs) are suitable materials to be included in Latent Thermal Energy Storage Systems (LTESS) to enhance the storage capacity per unit of volume. In order to increase their typical low thermal conductivity, PCMs are often loaded with high-porosity open-cell metal foams. Several correlations have been proposed in the literature to evaluate the effective thermal properties of the composite medium made of PCM and metal foam. However, the values of the effective thermal conductivity (k_{eff}) predicted by the different relationships can be very different from each other, with a consequent strong impact on the results of numerical simulations. In this work, a critical overview of the accuracy of the most used literature correlations for the evaluation of the effective thermal conductivity of open-cell metal-foam loaded PCMs is made: the temperature distribution obtained through a numerical model using different correlations is compared with the experimental values measured by testing different commercial paraffins loaded with copper or aluminum foams, subjected to complete melting. Since no correlation proves to yield accurate results for all the composite PCMs tested in this work, a new method for the calculation of the effective thermal conductivity of the PCM-metal foam medium is suggested.

Keywords

PCMs, paraffins, metal foams, porous media, conduction, effective thermal conductivity.

Nomenclature

Abbreviations

BA	Bhattacharya *et al.* correlation
BC	Boundary Condition
Exp	Experimental
HM	Homogeneous-medium model
HVAC	Heating, Ventilation and Air Conditioning
L	Lemlich correlation
LTESS	Latent Thermal Energy Storage Systems
M	Modified
MA	Mesalhy *et al.* correlation
MG	Maxwell Garnett correlation

PCM	Phase Change Material	
PL	Power Law model	
PM	Porous-medium model	
PPI	Pores Per Inch	
PR	Parallel model	
RES	Renewable Energy Sources	
SR	Series model	
TC	Thermocouple	
TESS	Thermal Energy Storage Systems	
WA	Wang *et al.* correlation	
WV	Weaver and Viskanta correlation	
Symbols		
A	Weight used in the Bhattacharya *et al.* correlation	
c_p	Specific heat capacity at constant pressure	[J/(kg·K)]
h	Convective heat transfer coefficient	[W/(m^2·K)]
H	Height from the polycarbonate case base	[m]
I	Current	[A]
k	Thermal conductivity	[W/(m·K)]
L	Latent heat of fusion / Characteristic length	[J/kg] / [m]
Q	Thermal power	[W]
Ra	Rayleigh number	
T	Temperature	[K]
t	Time	[s]
V	Voltage	[V]
z	Vertical coordinate	[m]
Greek symbols		
α	Mass fraction function	
β	Angle between heat flow direction and surface normal	[rad]
ε	Porosity	
θ	Phase indicator function	
μ	Dynamic viscosity	[Pa s]
ρ	Density	[kg/m^3]
Superscripts		
*	Fictitious	

Subscripts

a	Ambient air
eff	Effective
exp	Experimental
f	PCM
h	Heater
l	Liquid phase
m	Metal
max	Maximum
md	Middle of the phase change
min	Minimum
p1	Polycarbonate base
p2	Polystyrene base
pc	Phase change
S	Solid phase
Sim	Simulated

1. Introduction

The increase of the energy demand combined with the instability of the fossil fuels price is transforming the effort to optimize the use of Renewable Energy Sources (RES) in a mandatory priority, as highlighted by the European Commission targets fixed to 2030 [1]. To improve the RES use, the problem linked with their limited programmability has to be solved if one desires that the energy production from RES matches the instantaneous energy demand during the whole year. In order to solve this problem in RES-based HVAC systems, Thermal Energy Storage Systems (TESS) are usually introduced to tune energy production and demand [2]. Traditional TESS are sensible thermal energy storages consisting in water tanks that exploit the high thermal capacity of water in liquid phase. An interesting alternative to these systems is represented by Latent Thermal Energy Storage Systems (LTESS), where materials able to change phase within a desired temperature range (Phase Change Materials, PCMs) are suitably added in the water tank. In this case, not only the sensible heat accumulated in the material, but also the latent heat associated to the phase change is available for the storage of thermal energy, allowing to increase the storage capacity per unit of volume [2-6].

During the last decade, many research works have been devoted to the characterization of LTESS [3-6], whose applications can be found nowadays in many fields.

Among the different types of PCMs, paraffins are interesting for the application in LTESS thanks to a narrow temperature range of phase change, a high chemical inertness and non-toxicity [7]. On the other hand, all PCMs, and especially paraffins, are typically characterized by a low thermal conductivity value, which makes the heat charging and discharging times very high [8]. This reduces drastically the LTESS performance if the slowness of the heat transfer inside the PCM is not compatible with the characteristic times with which the stored heat must be made available to the user [9].

Therefore, many numerical and experimental studies have been focused on solutions able to increase the PCM thermal conductivity, such as the addition of metal inserts [10-12], nanoparticles [13-16], graphite [17,18], carbon fibers [19], periodic 3D metal structures [20-22], fins [23-27] and high porosity open-cell metal foams [7,9,28-34]. The latter solution has proved to be very effective in enhancing the conductive heat transfer inside the PCM thanks to the high thermal conductivity of the foam metal fibers [35], the high ratio of the foam surface in contact with the PCM and the foam volume, the highly interconnected structure and the natural mixing effect of fluids caused by the chaotic distribution of pores [9].

Due to the importance of improving PCM thermal conductivity to extend their use in LTESS, several works have been devoted to study numerically the thermal behavior of composite PCMs. An important direct effect linked to the increase of the "equivalent" thermal conductivity of the composite PCM, thanks to the use of metal foams or 3D-printed periodic solid materials, is the reduction of the charging and discharging times compared to the case of pure PCM. Alhusseny *et al*. [30] investigated the effects of loading a paraffin PCM with a copper foam in a LTESS demonstrating a 50% reduction in the PCM charging and discharging times. A similar result has been obtained by Chen *et al.* [34]; they studied numerically the heat transfer enhancement achievable by charging the paraffin PCM of a LTESS with a copper foam, obtaining, with different foam porosities, inlet flow rates and temperature, a 85% decrease of the PCM charging-discharging times, in comparison with pure PCM under specific operative conditions. The effect of the foam porosity on the charging/discharging times was investigated by Esapour *et al*. [7]; they studied a multi-pipe heat exchanger, analyzing the effects of the metal foam porosity, of the number of tubes and their layout on the performance of a LTESS. Their simulations show, in accordance with the experimental findings of Righetti *et al*. [36] and Rehman *et al*. [37], that charging and discharging times become shorter with the decrease of the foam porosity. Similar effects can be obtained by replacing metal

foams with 3D-printed periodic surfaces; Qureshi *et al.* [22] simulated a composite PCM made of a paraffin wax combined with different 3D-printed periodic surfaces and proved that the heat transfer coefficient increases and the PCM melting time can be reduced up to 30-40% compared to the case of pure PCM.

Mhiri *et al.* [38] studied, by means of numerical simulations made with COMSOL Multiphysics, the performance of a paraffin-graphite composite, embedded in a carbon foam by vacuum impregnation. The Authors investigated the effects of different porosity values and different volume fractions on the thermal conductivity of the composite PCM by obtaining that the addition of graphite and metal foam improves the material thermal conductivity up to 9 times with respect to the pure PCM.

The cited numerical works use for the analysis of the thermal behavior of pure or metal-foam loaded PCMs different approaches reviewed in [39] and [40]. In the *Enthalpy method*, for instance, the PCM latent and specific heat are combined into a non-linear enthalpy term in the energy equation, dependent on the current temperature value [41]; in the *Apparent heat capacity* formulation, the effect of the latent heat is taken into account by increasing the heat capacity term in the energy equation during the phase change [41-43]; in the *Source-based method*, specific heat and latent heat are separated and the latter is considered as a heat source term in the energy equation [44].

In addition, when a PCM is coupled to a metal foam, the choice of a numerical method able to accurately model the composite medium is needed. In this case, PCM and metal foam can be considered in local thermal equilibrium or in local thermal non-equilibrium [45,46].

It is well known that, in presence of heat transfer, models based on the assumption of local thermal non-equilibrium between solid and PCM generally give more accurate results [46] but this approach requires an additional computational effort and for this reason the models based on the local thermal equilibrium between solid and PCM are nowadays very popular and diffuse.

Under the hypothesis of local thermal equilibrium, the composite medium can be modeled by using a *Porous-medium* or a *Homogeneous-medium* approach.

In the *Porous-medium* model [47], the metal foam is modeled as a static solid and only the PCM changes phase in the composite medium. On the contrary, in the *Homogeneous-medium* model [48,49], the PCM and the metal foam are substituted by a new fictitious homogeneous phase change material, with intermediate effective properties between PCM and metal foam.

Both *Porous-medium* and *Homogeneous-medium* approaches need to associate to the medium fictitious “effective” thermophysical properties calculated on the basis of the PCM thermal properties

as well as the metal foam properties. Special attention must be paid in the evaluation of the effective thermal conductivity, whose value has a strong impact on the numerical results.

As an example, in COMSOL Multiphysics three different relationships are available to evaluate the effective thermal conductivity of the combination PCM-porous medium (k_{eff}) [50]: a porosity-weighted mean between the conductivity values of metal (k_m) and PCM (k_f) (corresponding to conduction in parallel); a weighted harmonic mean of k_f and k_m (corresponding to conduction in series); a weighted geometric mean of k_f and k_m (power law).

Some authors implemented in their numerical simulations effective thermal conductivity values for the composite PCMs that have been previously determined experimentally [51] using the thermal flux meter approach or the guarded hot plate approach or the transient plane source approach [52].

A series of correlations for the prediction of the k_{eff} value for metal foams filled with fluids have been proposed [28,53,54]. These correlations can be very useful for the evaluation of the effective thermal properties to be implemented as inputs in numerical simulations. Most correlations take into account the effect of the metal foam porosity on the effective thermal conductivity [35,48,49,55-58].

The available correlations for the evaluation of k_{eff} can be quite simple expressions (e.g. [57]) or more complex ones (e.g. [48,49]) and can be either explicit (e.g. [35,48,49,57]) or implicit (e.g. [58]); some correlations are derived from analytical models (e.g. [48]) and can include weight coefficients determined experimentally (e.g. [35]).

The prediction capability of the numerous correlations available in the open literature for the prediction of the effective thermal conductivity of the combination PCM-porous medium (k_{eff}) is strongly variable, as testified by comparisons with experimental results. At the moment, there is not a correlation recommended for the calculation of the effective properties of all the combinations metal foam-PCM. As an example, Inaba and Tu [59] measured the effective thermal conductivity of a paraffin PCM dispersed in a high density polyethylene foam at different temperature values, through a transient hot wire method. The Authors compared their results with the values of k_{eff} estimated with the correlation by Maxwell Garnett [55,56], by obtaining a maximum deviation of ±4.0% from the experimental results. Xiao *et al.* [60] measured the effective thermal conductivity of composite PCMs made of open-cell metal foams impregnated with pure paraffin by means of a steady-state test system. Their experimental outcomes in terms of k_{eff} values show a good agreement with the effective thermal conductivity values estimated by the correlation of Xu *et al.* [61]. Hong and Herling [62] performed experiments to investigate the effect of the surface area density of metal foams on the thermal conductivity of metal-foam loaded PCMs. The Authors found that the k_{eff} value estimated using the

porosity-weighted mean between the conductivity values of metal and PCM (conduction in parallel) can lead to some deviations from the experimental data, because the same porosity value can be obtained for metal foams with different surface area densities. The Authors evidenced the need of correlations for k_{eff} that take into account the surface area density effect. Zhang *et al.* [63] modeled the discharging cycles of a PCM coated in a spherical stainless steel shell both experimentally and theoretically. In order to predict the k_{eff} value of the composite PCM, they tested four different empirical correlations, detecting a 10% deviation of the different predicted values with respect to the experimental average value.

Siddiqui and Sun [64] calculated, by means of a finite element analysis, the effective thermal conductivity of microencapsulated phase change materials and compared their results with the theoretical predictions of Maxwell Garnett's model [55,56], obtaining a good agreement, dependent on the PCM volume fraction. Di Giorgio *et al.* [65] developed a mathematical model, solved in COMSOL Multiphysics, for a paraffin PCM loaded in a metal foam. They considered local thermal non-equilibrium and employed Lemlich's correlation [57] to evaluate the foam effective thermal conductivity. Their numerical results show a good match with previous experimental findings from the literature. Xu *et al.* [66] performed a numerical study for a composite material made of a paraffin wax loaded with different metal foams. The Authors evaluated the effective thermal conductivity k_{eff} of the composite PCM as a porosity-weighted mean between the conductivity values of metal and PCM and found a good agreement between their numerical results and experimental outcomes in terms of solid-liquid phase-change interface position.

Wu *et al*. [67] modeled the transport in complex porous media filled by single-phase and two-phase fluids by means of a new fractal theoretical model. The Authors derived an analytical expression for the effective thermal conductivity as a function of porosity, maximum pore diameter, tortuosity fractal dimension and fractal dimension.

Bianco *et al.* [68] employed a mathematical model based on volume-averaged porous media equations to evaluate the surface operation time of a finned heat sink with phase change material and metal foam, performing a multi-objective Pareto optimization with a genetic algorithm. The Authors considered a local thermal equilibrium approach and evaluated the stagnant thermal conductivity (that is summed to the thermal dispersion to obtain the effective thermal conductivity) employing the correlation by Bhattacharya *et al.* [35]. Venkateshwar *et al.* [69] derived empirical correlations to quantify the phase-change duration in foam-loaded PCMs. In these correlations, they employed Bhattacharya's relationship for the calculation of k_{eff} [35].

Rehman and Ali [37] investigated experimentally the effects of the PCM fraction and foam porosity on the thermal behavior of a paraffin PCM loaded with different metal foams. Also in this case Bhattacharya's correlation [35] was adopted to evaluate the composite PCM effective thermal conductivity.

In many experimental works cited above, the measured values are compared only with the numerical results obtained by calculating the effective thermal conductivity of the composite PCM using one specific correlation and a general conclusion about the reliability of the most cited correlations available in the literature is still missing.

However, a simple analysis of the values of the effective thermal conductivity of metal-foam loaded PCMs obtained by the most cited correlations for a fixed combination PCM-metal foam evidences how the k_{eff} values obtained selecting different relationships can be very different from each other, with differences up to 2 orders of magnitude.

For this reason, it is not surprising that the value of k_{eff} determined with a specific correlation proves to be accurate only for a particular composite PCM, but the same accuracy is not guaranteed when the PCM and/or the metal and/or the foam porosity is changed. As a consequence, it is expected that the choice of the correlation for the calculation of the thermal conductivity of a composite PCM can be crucial for an accurate modelling of the thermal behavior of an open-cell metal-foam loaded PCM.

The aim of this work is to make a critical overview of the accuracy of the most used literature correlations for the evaluation of the effective thermal properties of open-cell metal-foam loaded PCMs. The temperature distribution obtained through a numerical model implemented in COMSOL using different correlations is compared with the experimental values measured by testing different commercial paraffins (RT35 and RT35HC) loaded in copper or aluminum foams with similar porosity (95-96%) and different pore density (20 PPI (copper) and 10 PPI (aluminum)).

Indeed, the novelty of this work is to provide a quantitative analysis of the deviations between numerical results and experimental data obtained by adopting the most used correlations for four different composite PCMs (RT35 with copper foam, RT35 with aluminum foam, RT35HC with copper foam, RT35HC with aluminum foam) subjected to complete melting.

Finally, since no correlation proves to reproduce accurately the experimental evidence, a new simple method for the calculation of k_{eff} of metal-foam loaded PCMs is suggested, able to give accurate results for all the combinations metal foam-PCM considered in this work.

2. Experimental set-up

A dedicated experimental set-up has been built for the analysis of metal-foam loaded PCMs. The material to be tested is confined using a case, in the shape of a parallelepiped, made of polycarbonate (thermal conductivity 0.22 W/(m·K), density 1200 kg/m^3, specific heat capacity 1466 J/(kg·K)) with walls 0.05 m thick and internal dimensions of 0.145×0.1×0.09 m. An electric resistance is placed on the top of the case and is used to heat the PCM from above. A 0.06 m thick layer of polystyrene (thermal conductivity 0.06 W/(m·K), density 30 kg/m^3, specific heat capacity 1340 J/(kg·K)) is placed on each side of the case to provide thermal insulation (Figs. 1a,b).

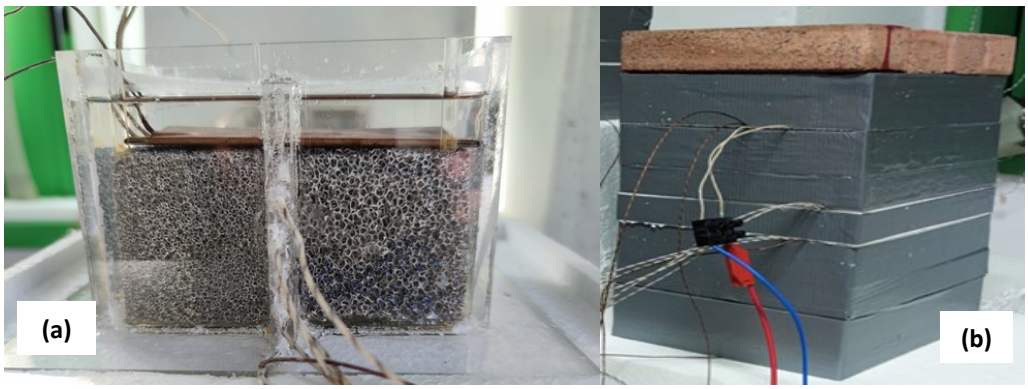

Fig. 1. Polycarbonate case filled with metal-foam loaded paraffin (a) and view of the external insulation jacket in polystyrene (b).

The electric heater is fed by means of a programmable power supply (*Mitek*, *mod. MKP3005D*); thanks to a relay controlled by an Arduino UNO® electronic board, the electrical loop can be opened or closed using a remote control. To measure the heat power generated by Joule effect, the ammeter and the voltmeter of the power supply are used. Five T-type thermocouples are placed at the center of the case at equally spaced distances from the bottom (TC_1-TC_5), in order to measure the vertical temperature distribution within the case (see Fig. 2). Two T-thermocouples (TC_h1 and TC_h2) are placed close to the bottom surface of the electric heater in contact with the PCM and another one is used to record the room temperature (TC_a). Two additional T-thermocouples are placed between the bottom surface of the polycarbonate case and the thermal insulation layer (TC_p1) and between the table and the external bottom surface of the polystyrene layer (TC_p2). In Fig. 2 a sketch with the position of each thermocouple is shown, with the indication of the distance (z) of each thermocouple from the bottom surface of the polycarbonate case.

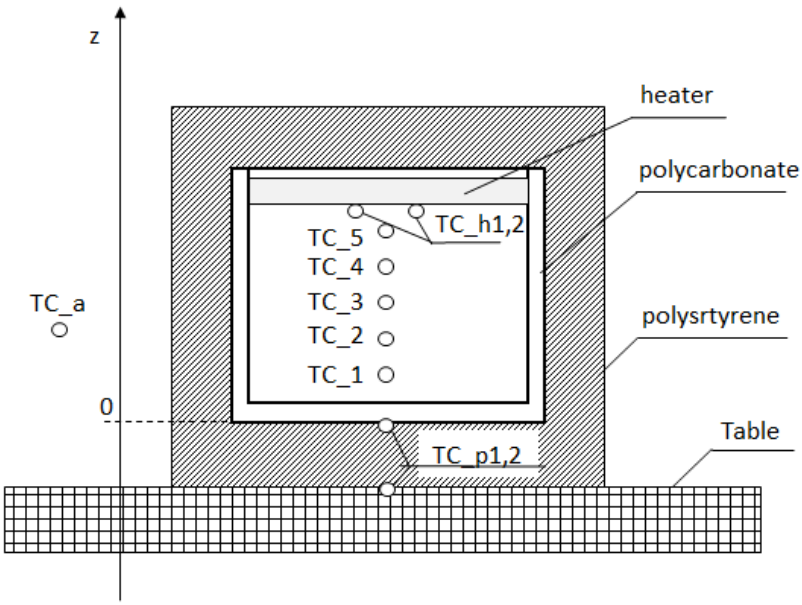

sensor	z [m]
TC_h1,2	0.070
TC_5	0.055
TC_4	0.042
TC_3	0.029
TC_2	0.016
TC_1	0.003
TC_p1	0
TC_p2	-0.060

Fig. 2. Name and position of the T-thermocouples.

The T-thermocouples are connected to a 9213 DAQ acquisition module (*National Instruments*, *US*), by means of which all the temperature measurements are managed with the help of LabVIEW in a PC. The lay-out of the complete test rig is shown in Fig. 3.

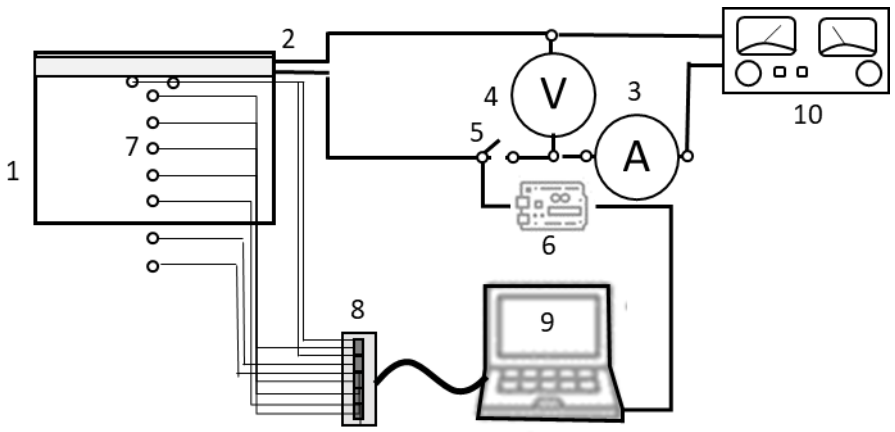

Fig. 3. Scheme of the experimental test rig: 1-Case; 2-Electrical heater; 3-Ammeter; 4- Voltmeter; 5-Relay; 6-Arduino UNO board; 7-T-thermocouples; 8-DAQ 9213; 9-PC; 10- Programmable power supply.

Two different commercial paraffin phase change materials have been tested, namely RT35 and RT35HC (*Rubitherm GmbH*, *D*). Both materials have similar thermophysical properties and melting

point, but RT35HC has a higher latent heat of fusion with respect to RT35 (+67%). In Table 1 the main thermal properties considered in this work are shown for the selected working materials.

Table 1. RT35 and RT35HC thermal properties.

PCM	Melting range [°C]	Latent heat of fusion [kJ/kg]	k [W/(m·K)]	ρ solid phase [kg/m^3]	ρ liquid phase [kg/m^3]	c_p solid phase [kJ/(kg·K)]	c_p liquid phase [kJ/(kg·K)]
RT35	30–39	138	0.2	860	770	3.4	2.0
RT35HC	33–37	230	0.2	880	770	2.0	2.0

A series of experimental runs have been made by testing metal-foam loaded PCMs. As demonstrated by many works appeared in the open literature, the presence of a metal foam is able to compensate the low thermal conductivity typical of PCMs (in this case k = 0.2 W/(m·K), see Table 1) and, as a consequence, to enhance the heat transfer. For this reason, in many applications PCMs are loaded with open-cell metal foams, either of copper or aluminum [7,9,28-34].

Samples of commercial aluminum (*Recemat*, *NL*) and copper (*Porometal*, *China*) foams with a similar declared porosity ε (i.e. ratio between the pores volume and the foam total volume, equal to 96% for aluminum and 95% for copper) have been used. The selected metal foams are characterized by different values of pore density (10 PPI for aluminum and 20 PPI for copper).

Both values of pore density and porosity have been verified for each specimen through different methods. The porosity of each sample has been measured by comparing the weight of the sample, measured by using an analytical balance (*RADWAG*, *mod. AS 220.R2*), with the expected weight of the volume filled by the solid material. The measured values of porosity confirm those declared by the manufacturer with a maximum deviation less than 1%. The pore density of each specimen has been verified by analyzing the topology of the surface of the metal foam samples with an automatic procedure based on the Image Toolbox of MATLAB. From the digital image of the surface, the pore contours are automatically individuated and the average value of the number of pores per unit of length of each specimen is calculated [70]. The obtained PPI values are in good agreement with the values declared by the manufacturer.

In Table 2 the main characteristics of the used open-cell metal foams are summarized.

Table 2. Summary of the main metal foams properties.

Material	Pore density [PPI]	Average pore dimension [mm]	Porosity [%]	k metal [W/(m·K)]	ρ metal [kg/m^3]	c_p metal [kJ/(kg·K)]
Copper	20	1.40	95	390	8920	385
Aluminum	10	2.55	96	237	2700	897

In order to couple PCM and metal foam, first the metal foams have been cut by a micro milling machine (*Roland MDX-40*) and inserted within the polycarbonate case, then the PCM in liquid phase has been poured in the container and left to cool at ambient temperature to reach the solid phase.

In each experimental run, the metal-foam loaded PCM is heated by the electric resistance from the top (see Figs. 1, 2 and 3), in order to avoid convection and have pure conductive heat transfer across the material. The distance of the heater from the case bottom is 0.071 m.

The power supplied by the electric resistance is controlled and maintained constant and equal to 3.1 W. In each run, the initial temperature of the system is very close to the room temperature (15-22°C during the test) which means that the PCM is fully solid at the beginning of each test. The experimental run is stopped when the PCM phase transition is completed and only liquid phase is present inside the case. The temperature measured by each thermocouple is recorded every 5 s. Each experimental run has been performed at least three times under the same operative conditions and the temperature measurements are compared to check the reliability of the experimental results.

In order to evaluate the accuracy of the measurements, the uncertainty associated to instruments is reported in Table 3. The uncertainty in the evaluation of the heat power Q is estimated after Moffat [71], starting from the uncertainty associated with the measurement of the single parameters involved in the calculation of Q (i.e. I and V) and results equal to ±0.1 W. About the uncertainty of the T-thermocouple, a calibration of the temperature sensors has been made in the range 15-70°C for comparison with a secondary reference platinum resistance thermometer (*Hart*, *mod. 5612*).

Table 3. Instrumentation and typical uncertainty.

Reference (Fig. 3)	Instrument	Field	Uncertainty
3	Ammeter	0 - 1 A	±0.01 A
4	Voltmeter	0 - 30 V	±0.1 V
7	T-thermocouple	0 - 200°C	±0.5 K

3. Numerical method

3.1 Modeling of composite phase change materials

The evolution of the temperature field within the polycarbonate case is studied by means of a 3D numerical model developed in COMSOL Multiphysics, able to reproduce the results obtained during the experimental runs. The real 3D geometry of the case is modeled as shown in Fig. 4.

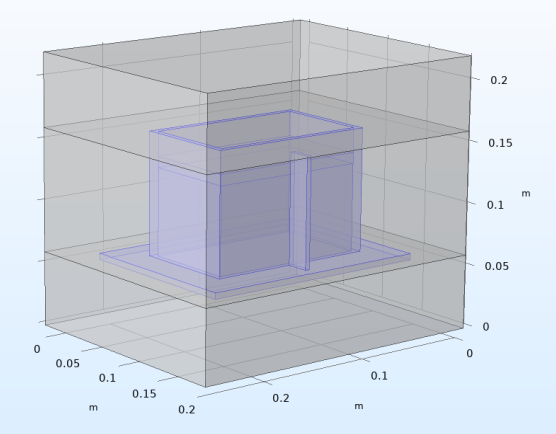

Fig. 4. 3D geometry of the computational domain.

The heat equation for a pure conductive problem without internal heat generation is used in COMSOL to reconstruct the temperature field within the working medium:

$$\rho c_p \frac{\partial T}{\partial t} = k\nabla^2 T \tag{1}$$

where (ρc_p) and k are the effective volumetric heat capacity and the effective thermal conductivity of the composite medium obtained by coupling PCM and metal foam: $(\rho c_p)_{eff}$ and k_{eff}.

For a metal-foam loaded PCM, the evaluation of the thermophysical properties which must be introduced in Eq. (1) becomes problematic, as underlined by many authors in the literature [28,53,54].

Two numerical approaches become possible: the adoption of the *Porous-medium* model [47] or the *Homogeneous-medium* one [48,49]. Both models take into account the metal foam porosity ε and assume a complete thermal equilibrium between the fluid (PCM) and the solid (metal foam).

In the *Porous-medium* (*PM*) model, the metal foam is considered as a static solid with constant thermal properties and only the PCM within the metal foam pores is involved in the phase change, that is modeled according to the apparent heat capacity formulation [41-43].

In the apparent heat capacity formulation, the phase change occurs within a temperature range ΔT_{pc}, centered on the temperature T_{md}, during which the PCM is neither solid nor liquid, but is in a transitional state with intermediate physical properties. The PCM density ρ_f is evaluated according to the equation:

$$\rho_f = \rho_s \theta + \rho_l \left(1-\theta\right) \tag{2}$$

where ρ_s is the density of the PCM solid phase, ρ_l is that of the PCM liquid phase and θ is the phase indicator function, that is equal to 1 if the temperature is lower than $T_{md} - \Delta T_{pc}/2$, decreases from 1 to 0 if the temperature is in the range $T_{md} - \Delta T_{pc}/2$ and $T_{md} + \Delta T_{pc}/2$ and is equal to 0 for temperature values higher than $T_{md} + \Delta T_{pc}/2$.

The PCM specific heat capacity at constant pressure, $c_{p,f}$, is evaluated as:

$$c_{p,f} = \left[\rho_s c_{p,s} \theta + \rho_l c_{p,l} \left(1-\theta\right)\right] \rho_f^{-1} + L \frac{\partial \alpha}{\partial T} \tag{3}$$

where $c_{p,s}$ is the specific heat capacity of the PCM solid phase, $c_{p,l}$ is that of the PCM liquid phase, L is the latent heat of fusion and α is the mass fraction function, defined as:

$$\alpha = \left[\rho_l \left(1-\theta\right) - \rho_s \theta\right] \left(2\rho_f\right)^{-1} \tag{4}$$

The PCM thermal conductivity k_f is obtained as an averaged weight of the thermal conductivity of the solid and liquid phase:

$$k_f = k_s \theta + k_l \left(1-\theta\right) \tag{5}$$

The PCM thermal properties are combined with those of the metal foam to obtain the effective thermal properties of the composite medium according to the *PM* model. In particular, the effective volumetric heat capacity, $(\rho c_p)_{eff}$, is evaluated as a porosity-weighted average of the volumetric heat capacity of the PCM ($\rho_f c_{p,f}$) and of the metal foam ($\rho_m c_{p,m}$):

$$\left(\rho c_p\right)_{eff} = \rho_f c_{p,f} \varepsilon + \rho_m c_{p,m} \left(1-\varepsilon\right) \tag{6}$$

In order to evaluate the effective thermal conductivity of the composite medium, k_{eff}, three different relationships are proposed in COMSOL. The first one (*PR relationship*) evaluates k_{eff} as a porosity-weighted mean between the conductivity values of metal (k_m) and PCM (k_f) (see *PM-PR* model in Table 4). The adoption of this relationship is justified when metal and PCM operate in parallel from a thermal point of view and the values of k_{eff} obtained following this way represent a physical upper bound for k_{eff}.

The second relationship (*SR*) is a weighted harmonic mean of the thermal conductivity of metal and PCM (see *PM-SR* model in Table 4). This relationship considers metal and PCM working in series and gives k_{eff} values which represent a physical lower bound for k_{eff}.

Finally, the third relationship (*PL*) is a power-law involving the weighted geometric mean of k_f and k_m (see *PM-PL* model in Table 4). This relationship provides good results if the two values of thermal conductivity associated to metal and PCM are similar; this is not the case for RT35 or RT35HC (k_f = 0.2 W/(m·K)) loaded with copper (k_m = 390 W/(m·K)) or aluminum (k_m = 237 W/(m·K)) foams.

Three simulations for each test have been generated by coupling the *Porous-medium* (*PM*) approach with these three relationships (i.e. *PM-PR*, *PM-SR*, *PM-PL*) in order to analyze which model gives results closer to the experimental ones.

In order to help the reader, Table 4 summarizes the equations used by each model (*PM-PR*, *PM-SR* and *PM-PL*) to evaluate $(\rho c_p)_{eff}$ and k_{eff}.

A different approach is used by the *Homogeneous-medium* (*HM*) model, which considers the composite material made of PCM and metal foam as a fictitious homogeneous material, with intermediate fictitious properties. In this case, all the material is subjected to the phase change, that is modeled according to the apparent heat capacity formulation.

In each phase, both the density ρ_{eff} and the specific heat capacity $c_{p,eff}$ of the homogeneous medium are evaluated as porosity-weighted averages between the values of metal and PCM, so the effective volumetric heat capacity of the composite medium, $(\rho c_p)_{eff}$, is obtained as follows:

$$\left(\rho c_p\right)_{eff} = \left[\rho_f \varepsilon + \rho_m \left(1-\varepsilon\right)\right]\left[c_{p,f} \varepsilon + c_{p,m} \left(1-\varepsilon\right)\right] \tag{7}$$

Different values of $(\rho c_p)_{eff}$ are obtained for the solid and liquid phase ($(\rho c_p)_{eff,s}$ and $(\rho c_p)_{eff,l}$, respectively) due to the different values of the PCM properties ρ_f and $c_{p,f}$ in the two phases. The

current value of $(\rho c_p)_{eff}$ is evaluated as a function of temperature according to Eqs. (2-4) (where the subscripts *f*, *s*, *l* are substituted by *eff*, *eff,s*, *eff,l*, respectively).

Different correlations have been proposed in the literature to evaluate the effective conductivity of the homogeneous medium. Maxwell Garnett [55,56] developed a homogenization theory (*MG*) according to which the effective thermal conductivity k_{eff} can be evaluated by using the correlation reported in Table 4 (see *HM-MG* model in Table 4).

Lemlich [57] proposed a simple expression for the evaluation of k_{eff} (*L*), valid for solid foams with low density and with a cell structure sufficiently open that approaches a lattice (see the *HM-L* model in Table 4).

Weaver and Viskanta [58] developed, through a mathematical model, an implicit relationship (*WV*) to determine k_{eff} (see the equations of the *HM-WV* model in Table 4).

Mesalhy *et al.* [48] deduced a more complex analytical equation (*MA*) by assuming one dimensional heat conduction (see the equations of the *HM-MA* model in Table 4).

Wang *et al.* [49] proposed a correlation (*WA*) that evaluates a value of k_{eff} which is intermediate between the values yielded by the *PR* and *SR* relationships (k_{max} and k_{min}, respectively), on the basis of the angle β between the heat flow direction and the surface normal (see the equations of the *HM-WA* model in Table 4). With the composite PCMs studied in the present paper, the angle β is nearly zero, so the value of the effective thermal conductivity according to the *WA* correlation is nearly coincident with k_{max} (*PR*).

Bhattacharya *et al.* [35] developed an empirical correlation (*BA*) that represents a weighted mean between the values given by the *PR* and *SR* relationships (see the equations of the *HM-BA* model in Table 4). The weight *A* of the correlation has been set by the authors equal to 0.35 through best fit of experimental data. This correlation, employed, among others, by Rehman and Ali [37] to evaluate the effective thermal conductivity of RT35HC loaded with copper and iron-nickel foams, is valid for foam porosities between 0.905 and 0.978 and pore densities between 5 and 40 PPI. The porosity and pore density of the metal foams considered in the present work fall within the ranges.

With each correlation, different values of k_{eff} are obtained for the solid and liquid phase if the PCM has different values of thermal conductivity in the solid and liquid phase (this is not the case of the PCMs considered in this work). The current value of k_{eff} is evaluated as a function of temperature according to Eq. (5) (where the subscripts *f*, *s*, *l* are substituted by *eff*, *eff,s*, *eff,l*, respectively).

Six models have been generated by coupling the *Homogeneous-medium* (*HM*) approach with the six relationships for the evaluation of k_{eff}: *HM-MG*, *HM-L*, *HM-WV*, *HM-MA*, *HM-WA*, *HM-BA*. In Table 4 the equations employed by each model to evaluate $(\rho c_p)_{eff}$ and k_{eff} are summarized.

A very first interesting observation is that, by using the typical properties of the commercial porous metal foams and PCMs tested in this work, the effective thermal conductivity values obtained by using the available correlations cited above are very different from each other.

In Table 5 the effective thermal conductivity values obtained for the composite material made by combining PCM (both RT35 and RT35HC) and the commercial copper or aluminum foams selected in this work are given. While some correlations (i.e. *PM-SR*, *PM-PL*, *HM-WV*) do not yield a significant change in the value of k_{eff} as the metal foam changes, others (i.e. *PM-PR*, *HM-MG*, *HM-L*, *HM-MA*, *HM-WA*, *HM-BA*) evidence a strong sensitivity to the properties of the metal foam, as evidenced by comparing the first with the second row of Table 5. In addition, for a fixed composite PCM, there exists a large difference between the values obtained selecting different relationships: the value of k_{eff} varies from 0.21 to 19.69 W/(m·K) and from 0.21 to 9.67 W/(m·K) for copper and aluminum foams, respectively (no differences between RT35 and RT35HC).

This means that it is expected that the choice of the relationship for the evaluation of k_{eff} has a significant impact on the results of the numerical model. It appears impossible that all these relationships can work accurately for the modelling of open-cell metal-foam loaded PCMs.

The main goal of this work is to make a benchmark of the relationships reported in Table 4 for the calculation of k_{eff} by comparing the temperature distribution obtained numerically using these relationships with the temperature distribution observed experimentally.

Table 4. Equations for the thermal properties of the composite PCM with the different models.

	$(\rho c_p)_{eff}$	k_{eff}	Model
PM	$\rho_f c_{p,f}\varepsilon + \rho_m c_{p,m}(1-\varepsilon)$ (6)	*PR*: $k_f\varepsilon + k_m(1-\varepsilon)$ (8)	*PM-PR*
		SR: $\left(\frac{\varepsilon}{k_f} + \frac{1-\varepsilon}{k_m}\right)^{-1}$ (9)	*PM-SR*
		PL: $k_f{}^{\varepsilon} + k_m{}^{1-\varepsilon}$ (10)	*PM-PL*
HM	$\left[\rho_f\varepsilon + \rho_m(1-\varepsilon)\right]\left[c_{p,f}\varepsilon + c_{p,m}(1-\varepsilon)\right]$ (7)	*MG*: $k_{eff} = k_m \frac{k_f(1+2\varepsilon) + 2k_m(1-\varepsilon)}{k_f(1-\varepsilon) + k_m(2+\varepsilon)}$ (11)	*HM-MG*
		L: $k_{eff} = k_m \frac{1-\varepsilon}{3}$ (12)	*HM-L*
		WV: $k_{eff} = k_m - \left(\frac{k_{eff}}{k_f}\right)^{1/3}(k_m - k_f)\varepsilon$ (13)	*HM-WV*
		MA: $k_{eff} = \frac{\left[k_f + \pi\left(\sqrt{\frac{1-\varepsilon}{3\pi}} - \frac{1-\varepsilon}{3\pi}\right)(k_m - k_f)\right]\left[k_f + \frac{1-\varepsilon}{3}(k_m - k_f)\right]}{k_f + \left[\frac{4}{3}\sqrt{\frac{1-\varepsilon}{3\pi}}(1-\varepsilon) + \pi\sqrt{\frac{1-\varepsilon}{3\pi}} - (1-\varepsilon)\right](k_m - k_f)}$ (14)	*HM-MA*
		WA: $k_{eff} = \sqrt{k_{\max}^2\cos^2\beta + k_{\min}^2\sin^2\beta}$; $\tan^2\beta = 16(1-\varepsilon)\varepsilon^3\frac{\ln(k_m/k_f)}{(k_m/k_f - 1)^2}$ (15)	*HM-WA*
		BA: $A\left[k_f\varepsilon + k_m(1-\varepsilon)\right] + (1-A)\left(\frac{\varepsilon}{k_f} + \frac{1-\varepsilon}{k_m}\right)^{-1}$ (16)	*HM-BA*

Table 5. Effective thermal conductivity values [W/(m·K)] obtained by using different relationships quoted in the open literature for metal-foam loaded PCMs (RT35 or RT35HC)

Foam	*PM-PR*	*PM-SR*	*PM-PL*	*HM-MG*	*HM-L*	*HM-WV*	*HM-MA*	*HM-WA*	*HM-BA*
Copper (ε=95%, PPI= 20)	19.69	0.21	1.56	13.42	6.50	0.23	7.73	19.69	7.03
Aluminum (ε=96%, PPI=10)	9.67	0.21	1.46	6.60	3.16	0.23	3.82	9.67	3.52

3.2 Validation of the thermal boundary conditions

First of all, a validation of the numerical model in COMSOL has been done. The temperature distribution within the computed volume obtained numerically depends not only on the properties of the medium (i.e. (ρc_p) and k) but also on the imposed thermal boundary conditions. If the goal is to use the numerical model to reproduce the experimental results, it becomes mandatory to know what kind of thermal boundary conditions have to be adopted by the numerical model.

In order to decouple the effect of the imposed thermal boundary conditions from that of the thermal properties, a special experimental run has been made by filling the case with pure demineralized water. In this case, the values of the thermal properties of the fluid ((ρc_p) and k) are known, so the temperature distribution within the case depends only on the imposed thermal boundary conditions. In addition, in this test only liquid water is involved under a pure conduction regime. Water is heated by the electric resistance for about 9 h, then the thermal power is switched off and water is cooled down for additional 21 h. Eq. (1) has been solved in COMSOL by considering the thermal conductivity and volumetric heat capacity of pure water in order to validate the imposed thermal boundary conditions by comparison with the experimental results.

The 3D computational domain has been discretized through an unstructured tetrahedral mesh with about 300 000 elements, with minimum element size 0.4 mm and maximum one 9 mm (Fig. 5). The mesh independence of the results has been checked observing that the maximum discrepancy in terms of temperature values obtained by varying from 300 000 to 1 400 000 the number of the 3D mesh elements is about 0.2 K, less than the temperature measurement uncertainty.

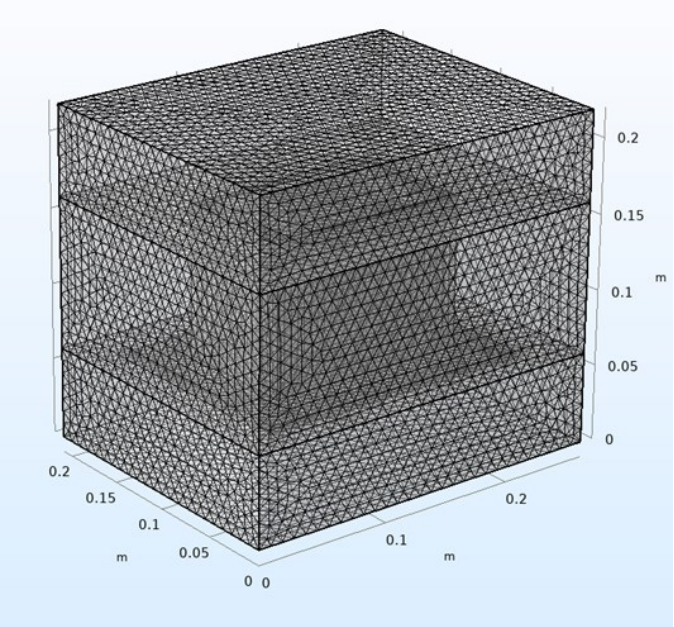

Fig. 5. 3D computational mesh.

On the top and lateral surfaces of the computational domain, a third-order thermal boundary condition is imposed by considering external natural convection with air. The room temperature recorded by the thermocouple TC_a (see Fig. 2) is implemented as time-dependent temperature of air. The convective heat transfer coefficient h is calculated by COMSOL as a function of the Rayleigh number by means of correlations validated for horizontal and vertical plates [72]. For the top surface of the case, h is evaluated as:

$$\begin{aligned} h &= \frac{k}{L} 0.54 Ra_L^{1/4} \quad \text{if } 10^4 \le Ra_L \le 10^7 \\ h &= \frac{k}{L} 0.15 Ra_L^{1/3} \quad \text{if } 10^7 \le Ra_L \le 10^{11} \end{aligned} \tag{17}$$

where k is the air thermal conductivity and L is the wall characteristic length (area/perimeter). For the lateral surfaces of the case, h is calculated as:

$$h = \frac{k}{L}\left\{0.68 + \frac{0.67 Ra_L^{1/4}}{\left[1+\left(\frac{0.492k}{\mu c_p}\right)^{9/16}\right]^{4/9}}\right\} \quad \text{if } Ra_L \le 10^9$$

$$h = \frac{k}{L}\left\{0.825 + \frac{0.387 Ra_L^{1/6}}{\left[1+\left(\frac{0.492k}{\mu c_p}\right)^{9/16}\right]^{8/27}}\right\} \quad \text{if } Ra_L > 10^9 \tag{18}$$

where the characteristic length L is the wall height.

The obtained values of the convective heat transfer coefficient (h) range from 1.49 to 3.43 W/(m^2·K) by considering the geometry of the case and the air temperature range. On the bottom surface of the domain, the time-dependent temperature measured by the thermocouple TC_p2 (see Fig. 2) has been imposed. As initial condition, the mean of the temperature values measured at the initial time by the thermocouples inserted within the case has been adopted for the whole domain. In order to simulate the heat supplied by the electric resistance, the time-dependent temperature TC_h evaluated as the average between the values measured by the two thermocouples next to the heater (i.e. TC_h1 and TC_h2, see Fig. 2) has been imposed in correspondence of the position of the electric heater in the computational domain. Table 6 summarizes the imposed boundary conditions adopted in the numerical model.

Table 6. Imposed thermal boundary conditions (BC) for the numerical model.

External surface	Boundary condition
Bottom surface	First-order BC: imposed time-dependent temperature (TC_p2)
Lateral surfaces (×4)	Third order BC: time-dependent natural convection with air (using TC_a)
Top surface	Third order BC: time-dependent natural convection with air (using TC_a)
Heating resistance	First-order BC: imposed time-dependent temperature (TC_h)

The simulation is performed for 30 h by selecting a relative tolerance equal to 10^{-4} and an absolute tolerance equal to 10^{-5}. The time required to run the simulation is 7 min on a PC with Intel Core i7-6700K 4.0 GHz, RAM 64 GB. The time-dependent temperature of water has been evaluated in

correspondence of the positions of the five thermocouples inserted within the case (TC_1-TC_5) and in correspondence of the position of the thermocouple at the bottom of the polycarbonate case (TC_p1). The results of the 3D numerical simulation are compared with the experimental outcomes in Fig. 6.

From Fig. 6 it is evident how the findings of the numerical simulation reproduce well the experimental behavior: the maximum deviation between numerical and experimental values, in terms of temperature, is equal to 0.7 K, but 74% of the temperature values differ from the experimental ones less than the thermocouple uncertainty, so that the thermal boundary conditions can be considered validated.

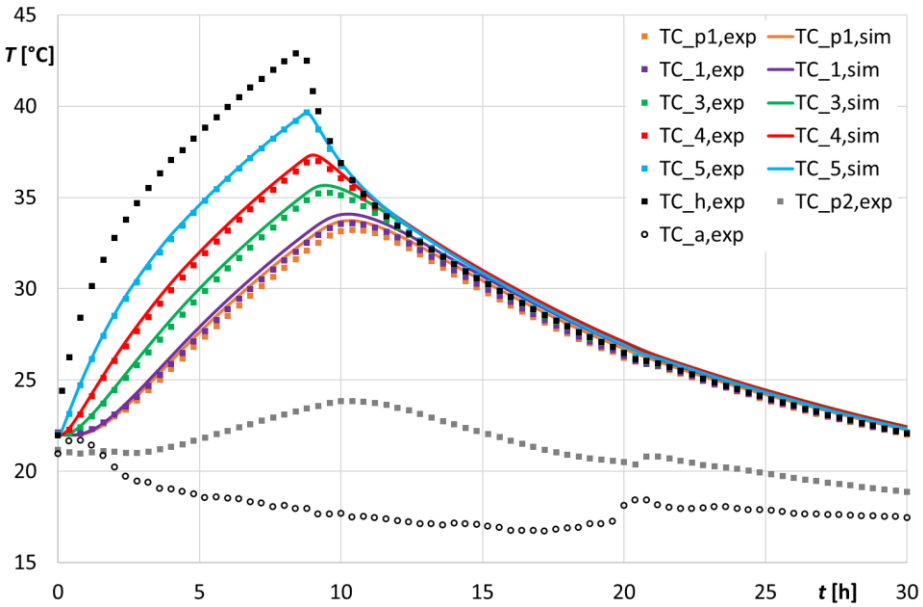

Fig. 6. Temperature as a function of time, case filled with water: thermocouples within water (TC_1-TC_5), polycarbonate base (TC_p1), heater (TC_h), polystyrene base (TC_p2), ambient air (TC_a), experimental (exp) vs simulated (sim).

4. Results and discussion

4.1 Results with different numerical models

Once validated the numerical model, a series of simulations have been performed in COMSOL Multiphysics with the aim to test different approaches for the modeling of PCMs loaded with metal foams by comparing the capability of each approach to reproduce the experimental behavior of four different foam-loaded PCMs: RT35 loaded with copper foam, RT35 loaded with aluminum foam,

RT35HC loaded with copper foam, RT35HC loaded with aluminum foam. The 3D model with the same mesh and tolerance values reported in Section 3.2 has been employed.

In order to compare the results obtained with the different models to each other and to the experimental outcomes, it is useful to plot the temperature trends for one thermocouple. Fig. 7 shows the time-dependent temperature values in correspondence of the position of the thermocouple in the middle of the case (TC_3, at 0.029 m from the case base, see Fig. 2), for RT35 loaded with copper foam, obtained experimentally and numerically. In Fig. 7a the *Porous-medium* model has been adopted by considering, for the evaluation of the effective thermal conductivity, correlations validated for conduction in parallel (*PM-PR*), in series (*PM-SR*) or adopting a power law relationship (*PM-PL*). From Fig. 7a it is evident how the models *PM-SR* and *PM-PL* predict a very low effective thermal conductivity for the medium (0.21 and 1.56 W/(m·K), respectively); these low values are not able to correctly reproduce the experimental outcomes. In both cases, the numerical values (orange and purple lines of Fig. 7a) are significantly lower (up to 11.3 K) than those obtained by the experimental tests (black markers in Fig. 7a). This means that PCM and metal foam do not act, from a thermal point of view, as two materials in series. The composite material behavior cannot even be described by a power law, since the thermal conductivity of metal is strongly higher than that of PCM. On the other hand, the numerical results given by the *PM-PR* model (green dashed line in Fig. 7a) are more similar to the experimental ones (black markers), but always larger. In addition, this model anticipates the beginning of the pure-liquid phase, identified by the second slope change in the temperature curve. Both effects highlight how the *PM-PR* model tends to overestimate the effective thermal conductivity (in this case k_{eff} is equal to 19.69 W/(m·K)).

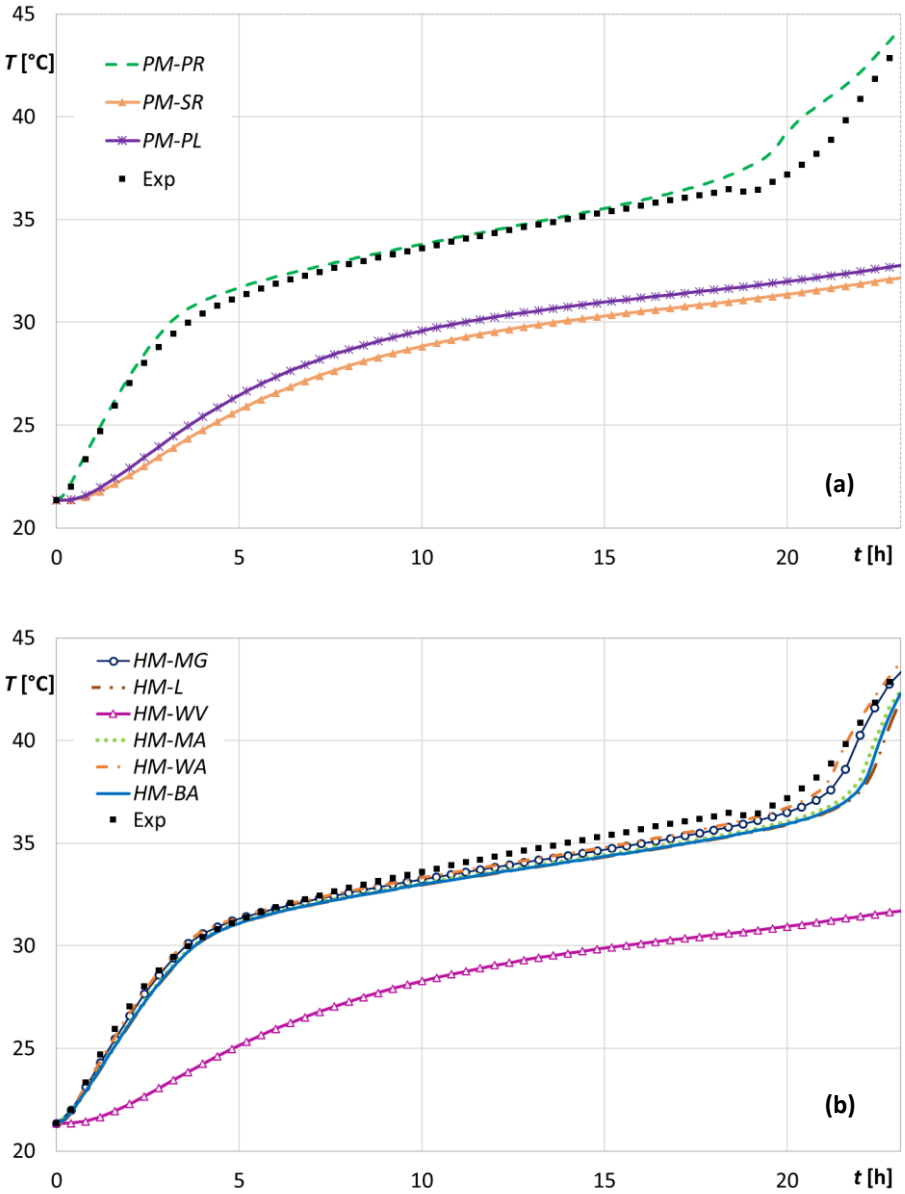

Fig. 7. Temperature of thermocouple TC_3 as a function of time, RT35 loaded with copper foam, experimental data vs numerical results adopting: a) the *Porous-medium* model, b) the *Homogeneous-medium* model.

Fig. 7b compares the experimental temperature values recorded by TC_3 with the numerical ones obtained by using the *Homogeneous-medium* model adopting different correlations for the calculation of k_{eff}. The *HM-WV* model strongly underestimates the effective thermal conductivity (k_{eff} = 0.23 W/(m·K)) and, as a consequence, strongly underestimates the temperature values with respect to the experimental ones. The other correlations yield results more similar to the experimental ones, but almost always lower, especially at the end of the phase change as well as in the pure liquid phase.

The differences between the results of the different models can be easily appreciated by observing the end of the phase change zone, when the PCM is completely liquified (note that RT35 melting range is 30–39°C). From Fig. 8 it is evident that the beginning of the pure liquid phase is a critical region and that only the *HM-WA* model (orange dash and dot line, k_{eff} 19.69 W/(m·K)) is able to reproduce the experimental curve quite well. In addition, in the pure liquid phase some differences, up to 1.3 K, appear between the temperature values evaluated by the *HM-L*, *HM-MA* and *HM-BA* models (brown dash-dot-dot, green dotted and blue solid lines, respectively and k_{eff} from 6.50 to 7.73 W/(m·K)), whereas in the previous phases they yielded nearly coincident results. Indeed, the end of the melting phase is a challenging region to reproduce through numerical simulations, because the combined effects of the accuracy in the estimation of the effective thermal conductivity, latent heat of fusion and specific heat capacity in liquid phase influence the results.

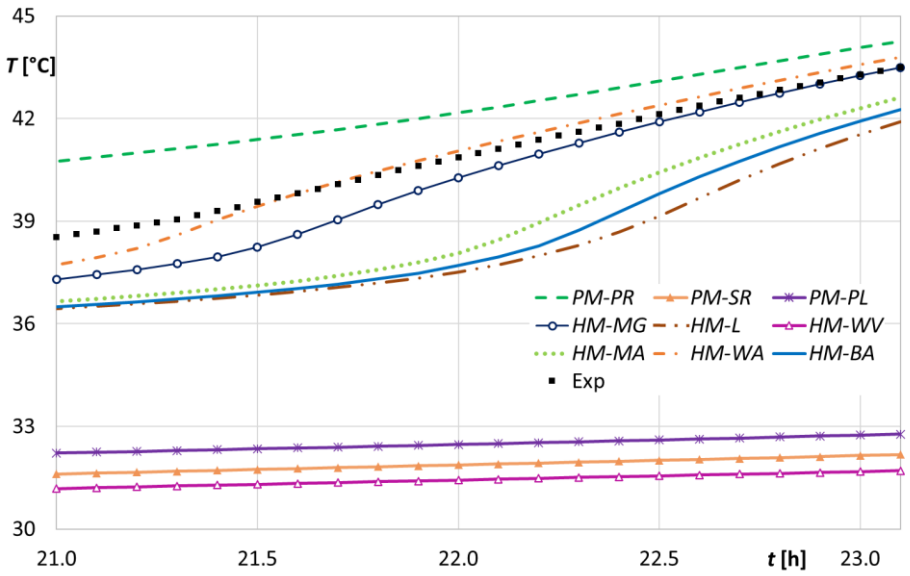

Fig. 8. Temperature of thermocouple TC_3 as a function of time, focus on the liquid phase; RT35 loaded with copper foam, experimental vs numerical data.

Another consideration that can be derived from Fig. 8 is that using the same value of k_{eff} with different models (*Porous-medium* vs *Homogeneous-medium*) yields different results, as can be drawn by comparing the temperature trends of the *PM-PR* model (green dashed curve) with those of the *HM-WA* model (orange dash and dot line): in both cases k_{eff} = 16.69 W/(m·K), but the first model overestimates the temperature values, while the second one underestimates them for most of the time.

In order to quantify the deviations from the experimental trend, Table 7 shows the maximum temperature differences, with respect to the experimental outcomes, obtained in correspondence of TC_3 by each numerical model. The temperature differences are reported separately for the three main heating zones (i.e. solid phase, phase change and liquid phase) and for the four composite PCMs. The maximum deviations are obtained almost always in the liquid phase, where a difference from the experimental values up to -13.8 K is reached (*PM-SR* and *HM-WV* models for RT35 loaded with aluminum foam). An important result that can be deduced by observing Table 7 is that there is not a numerical model that gives the best results for all the composite PCMs considered.

Indeed, the *Homogeneous-medium* model with the correlation by Wang et al. [49] (*HM-WA* model) yields the minimum deviation from the experimental results both for RT35 and RT35HC loaded with copper foam, but the *Homogeneous-medium* model with the correlation by Mesalhy et al. [48] (*HM-MA* model) proves to perform better for RT35 loaded with aluminum foam, whereas the *Homogeneous-medium* model either with the correlation by Mesalhy et al. [48] or by Bhattacharya et al. [35] (*HM-MA* model and *HM-BA* model, respectively) is the best choice for RT35HC loaded with aluminum foam.

The results presented up to now refers to the temperature values evaluated in correspondence of the thermocouple TC_3, namely the sensor in the middle of the case, in order to make the comparison between the results of the different numerical models easier. However, in order to have a complete view on the accuracy of the different models, the temperature evaluated in correspondence of each thermocouple must be taken into account, since an optimal agreement with the experimental values in correspondence of the central sensor does not guarantee a similar behavior in correspondence of the thermocouples at the top and/or at the bottom of the case. For this purpose, in Fig. 9 the temperature distribution along the case height is plotted for fixed instants of time.

Table 7. Maximum absolute deviation [K] in each phase (TC_3) with the numerical models from the literature (*PM-PR – HM-BA*) and with the new *Modified Porous-medium* model (*PM-M*).

Composite PCM	Model	*PM-PR*	*PM-SR*	*PM-PL*	*HM-MG*	*HM-L*	*HM-WV*	*HM-MA*	*HM-WA*	*HM-BA*	*PM-M*
RT35 + copper	Solid phase	0.7	-5.6	-5.0	-0.5	-0.9	-6.1	-0.8	-0.4	-0.8	0.3
	Phase change	2.3	-7.4	-6.8	-1.3	-2.4	-7.8	-2.1	-0.8	-2.3	1.1
	Liquid phase	1.9	-11.3	-10.7	-1.3	-3.4	-11.8	-2.8	0.3	-3.2	1.1
RT35 + aluminum	Solid phase	1.6	-4.9	-4.4	1.3	0.6	-4.8	0.8	1.5	0.7	0.8
	Phase change	3.1	-6.9	-6.5	2.1	-1.2	-6.9	0.7	2.8	-1.0	0.7
	Liquid phase	2.5	-13.8	-13.1	2.0	-1.4	-13.8	-0.3	2.4	-1.0	0.6
RT35HC + copper	Solid phase	1.8	-4.3	-3.7	1.4	1.2	-4.7	1.2	1.5	1.2	1.4
	Phase change	3.2	-4.2	-3.8	-1.5	-1.7	-4.4	-1.7	-1.4	-1.7	-0.6
	Liquid phase	3.2	-9.3	-8.9	-4.6	-6.1	-9.6	-5.8	-4.0	-5.9	0.9
RT35HC + aluminum	Solid phase	2.6	-4.1	-3.6	2.5	1.9	-4.0	2.1	2.6	2.0	2.0
	Phase change	4.1	-4.2	-3.8	3.0	-0.9	-4.2	0.6	3.8	-0.6	0.6
	Liquid phase	3.9	-13.4	-12.9	3.2	-1.8	-13.4	1.1	3.8	-0.8	1.7

In Fig. 9 the temperature values recorded by each thermocouple (black markers) are compared with those evaluated numerically by using different ways to estimate the medium properties, in correspondence of the most critical time instants, namely at the beginning and at the end of the phase change (whose temperature range is highlighted in the graphs through vertical dotted lines). For each composite PCM, the results of the *Porous-medium* and *Homogeneous-medium* models that yielded the smallest deviations with respect to the experimental values have been plotted, i.e. *PM-PR* (green dashed lines), *HM-WA* (orange solid lines), *HM-BA* (blue solid lines) and *HM-MA* (green solid line). From the plots it is evident that, while in some cases the deviation in terms of temperature due to the estimation of the medium properties is nearly constant along the case vertical axis (i.e. blue line and black markers on the right side of the graph in Fig. 9b), in others the error is minimal for the bottom thermocouple but gradually increases with the thermocouple distance from the bottom of the case (i.e. orange line and black markers on the right side of the graph in Fig. 9a); in this case a temperature difference of -0.02 K is observed in correspondence of the bottom thermocouple (TC_1) and this difference becomes equal to -1.7 K in correspondence of the top one (TC_5). In other cases, the deviation decreases with the thermocouple distance from the bottom (i.e. blue line and black markers on the left side of the graph in Fig. 9b). These trends can be explained by observing the effective thermal conductivity values associated to the medium adopting the different correlations (see Table 5); when a large effective thermal conductivity is associated to the medium, the temperature

difference between the bottom and the top thermocouple is reduced because the heat transfer across the medium is strongly enhanced (i.e. *PM-PR* model) and the end of the phase change is anticipated with respect to the experimental evidence.

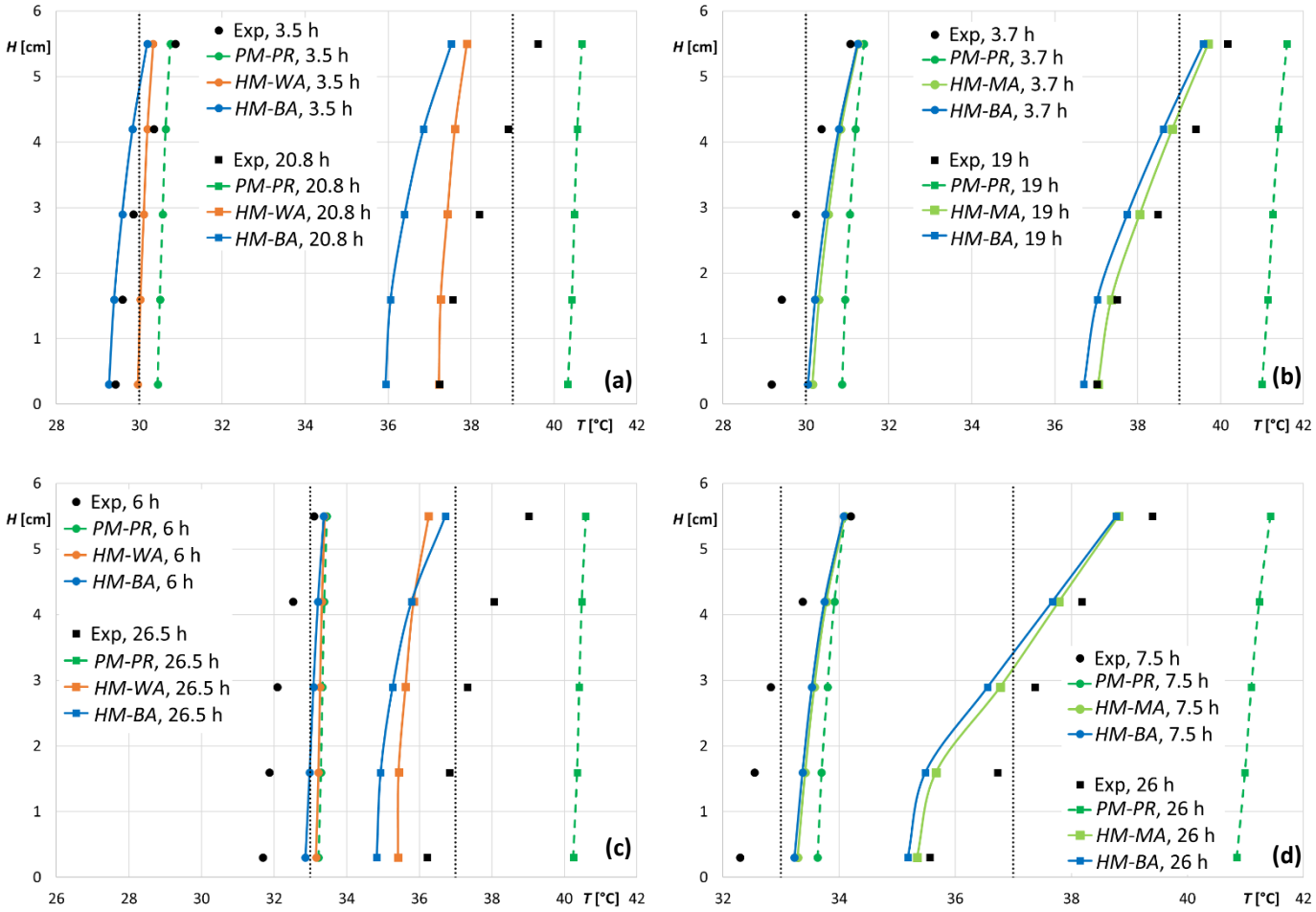

Fig. 9. Constant-time curves as functions of height (H) and temperature (T), recorded by the thermocouples and evaluated numerically with selected models, RT35 with copper (a), RT35 with aluminum (b), RT35HC with copper (c), RT35HC with aluminum (d).

From Fig. 9 it is also possible to appreciate how the use of a porous metal, with consequent increase in thermal conductivity with respect to pure PCM, enhances the heat transfer: the temperature difference between the top and the bottom thermocouples does not exceed 4 K for all the tested combinations PCM-metal foams, evidencing a quite uniform temperature distribution within the material.

4.2 New simplified model

In the classical approach, in order to model numerically a metal foam-loaded PCM, the values of thermal conductivity of porous solid medium and PCM are used together with the porosity of the solid medium to obtain the effective thermal conductivity value.

The results shown in this paper highlight how many of the relationships found in the open literature can bring to very large or very low values of effective thermal conductivity, not realistic by considering the experimental evidence.

As an example, it is easy to demonstrate how the classical *SR* relationship is able to generate very low values of the effective thermal conductivity if a porous media having a high porosity ($\varepsilon \approx 1$) is considered. In fact,

$$k_{eff} = \lim_{\varepsilon \to 1} \left(\frac{\varepsilon}{k_f} + \frac{1-\varepsilon}{k_m} \right)^{-1} = k_f \tag{19}$$

Under the conditions of this work (ε = 95% for copper and ε = 96% for aluminum), the effective thermal conductivity k_{eff} obtained by using the *SR* relationship remains nearly coincident with the value of the PCM thermal conductivity (0.2 W/(m·K) for both RT35 and RT35HC), independently of the thermal conductivity of the porous foam; this result is not confirmed by the experimental observations.

If one uses the *PL* relationship (see Table 4), the weight of k_m in the k_{eff} evaluation is low when high values of the metal foam porosity are considered and, as a consequence, a change in the thermal conductivity of the metal foam does not lead to a very different value of the effective thermal conductivity, which is in disagreement with the experimental data.

With the aim to solve this mismatch with the experimental evidence, Bhattacharya *et al.* [35] proposed to calculate the effective thermal conductivity of a PCM loaded with a metal foam by using a weighted mean of *SR* and *PR* relationships:

$$k_{eff} = A \left[k_f \varepsilon + k_m (1-\varepsilon) \right] + (1-A) \left(\frac{\varepsilon}{k_f} + \frac{1-\varepsilon}{k_m} \right)^{-1} \tag{20}$$

where A is a weight factor deduced by the experimental results. The A value proposed by Bhattacharya *et al.* [35] is equal to 0.35. However, if Eq. (20) is used in presence of high porosity metal foams ($\varepsilon \approx 1$), one can observe, combining Eq. (19) with Eq. (20), that:

$$k_{eff} \simeq A\left[k_f \varepsilon + k_m\left(1-\varepsilon\right)\right] + \left(1-A\right)k_f \tag{21}$$

After some algebra, in presence of a high metal foam porosity (ε almost equal to 1), the expression of Bhattacharya's correlation for the effective thermal conductivity estimation can be written as follows:

$$k_{eff} \simeq A\, k_m\left(1-\varepsilon\right) + \varepsilon k_f \tag{22}$$

In this way, Bhattacharya's correlation is reconducted to a *PR* relationship in which the thermal conductivity of the solid foam is modified through a scaling factor A.

The simplified version (Eq. (22)) of Bhattacharya's correlation can be used directly in COMSOL (where the user can only select among *SR*, *PL* and *PR* relationships for the evaluation of the effective thermal conductivity of a metal-foam loaded PCM).

Modified values of thermal conductivity for copper and aluminum have been implemented in the *PM-PR* model: a fictitious thermal conductivity ($k_m^* = A\, k_m$) equal to 136.5 and 82.95 W/(m·K) for copper and aluminum, respectively, has been used.

The results of the proposed simplified model based on Eq.(22), called here *Modified Porous-medium* model (*PM-M*), obtained in correspondence of the middle thermocouple for each composite medium, are plotted in red in Fig. 10, together with the temperature trends of the most accurate *PM* and *HM* models from the literature. It is possible to appreciate from Fig. 10 how the numerical predictions obtained using the *PM-M* model show an optimal agreement with the experimental temperature values, for all the four composite PCMs. The root mean square deviation in terms of temperature (equal to 0.3, 0.3, 0.7 and 0.8 K for RT35 with copper, RT35 with aluminum, RT35HC with copper and RT35HC with aluminum, respectively) is lower than that obtained from the best literature models. In the last column of Table 7, the maximum deviations of the *PM-M* model results from the experimental outcomes in the solid phase, the phase change and the liquid phase is reported for the four composite PCMs. By comparing these values with those obtained by using the other approaches, it is evident that the accuracy of the *PM-M* model is comparable to that of the most accurate existing models, namely *HM-WA* for the copper-foam loaded PCMs and *HM-MA* for the aluminum-foam loaded PCMs, with the advantage of using a single model able to provide accurate results for each composite medium.

The quality of the *PM-M* model results is due to the combination of: i) an accurate estimation of the k_{eff} value: the correlation by Bhattacharya *et al.* [35] is a weighted mean between the values of conduction in parallel and in series, where the weight A is experimentally determined; ii) a precise

numerical approach: the *Porous-medium* model considers a porous metal solid filled with a fluid (PCM), where only the latter is able to change phase.

Some deviations from the experimental results (up to 2 K) can be still observed at the beginning of the phase change of RT35HC (Fig. 10c-d). In order to eliminate these discrepancies, temperature-dependent values of the PCM thermal properties (i.e. specific heat capacity) have to be considered for these particular paraffine PCM.

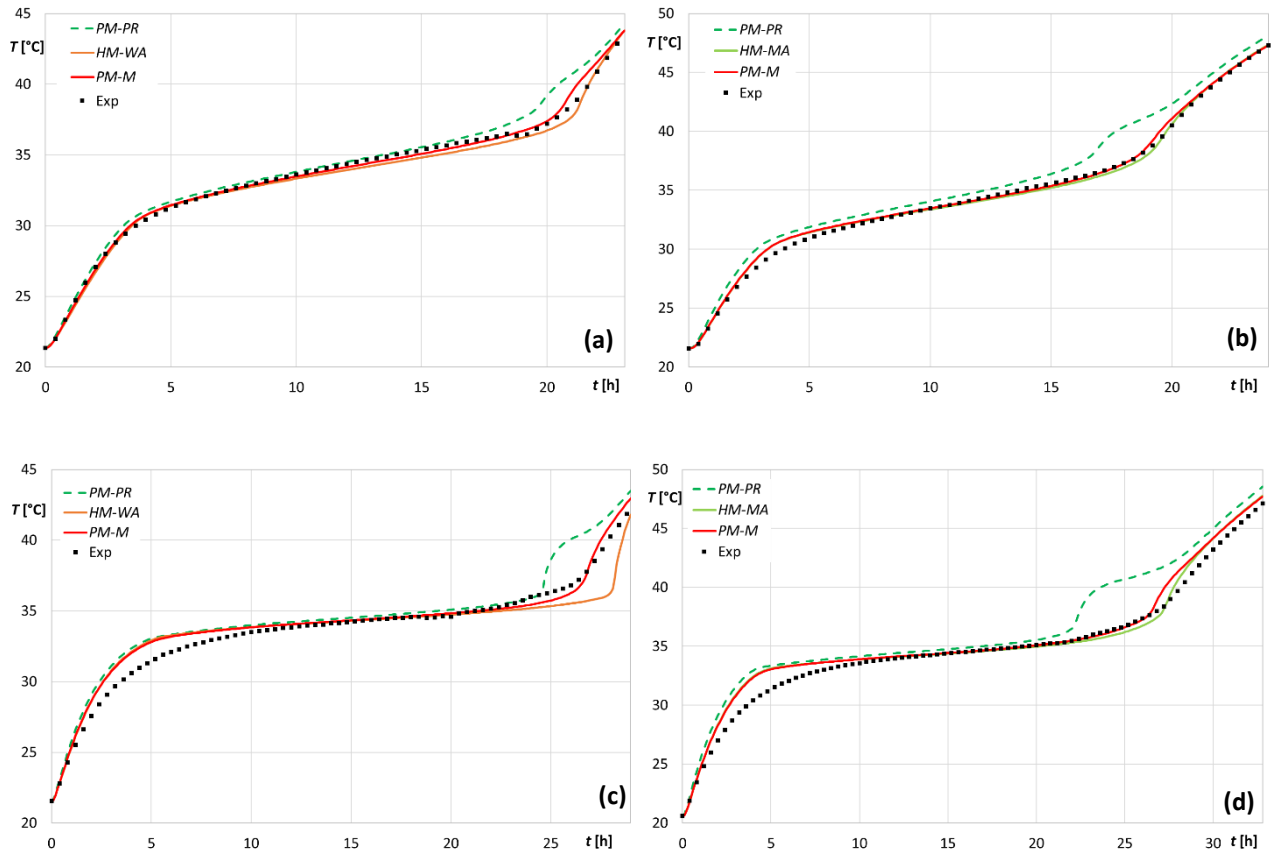

Fig. 10. Temperature of thermocouple TC_3 as a function of time, RT35 with copper (a), RT35 with aluminum (b), RT35HC with copper (c), RT35HC with aluminum (d), experimental data vs numerical results with selected literature models and *Modified Porous-Medium* model.

Fig. 11 compares the temperature values given by the *PM-M* model and by selected literature models, in correspondence of each thermocouple of the case, at the two instants corresponding to the beginning and end of the phase change. For each metal-foam loaded PCM, the *PM-M* model (red curves in Fig. 11) provides temperature values quite close to the experimental ones (black markers in Fig. 11), but in some cases consistent deviations can be still observed for the lower thermocouples, e.g. at the end of the phase change for RT35 loaded with copper foam (see Fig. 11a), where the

discrepancy for the bottom thermocouple reaches 1.3 K. Nevertheless, even in these cases the deviations are lower than or similar to those of the most accurate literature models (i.e. *HM-WA* for copper-foam loaded PCMs (orange lines in Fig. 11a,c) and *HM-MA* for aluminum-foam loaded ones (green solid lines in Fig. 11b,d).

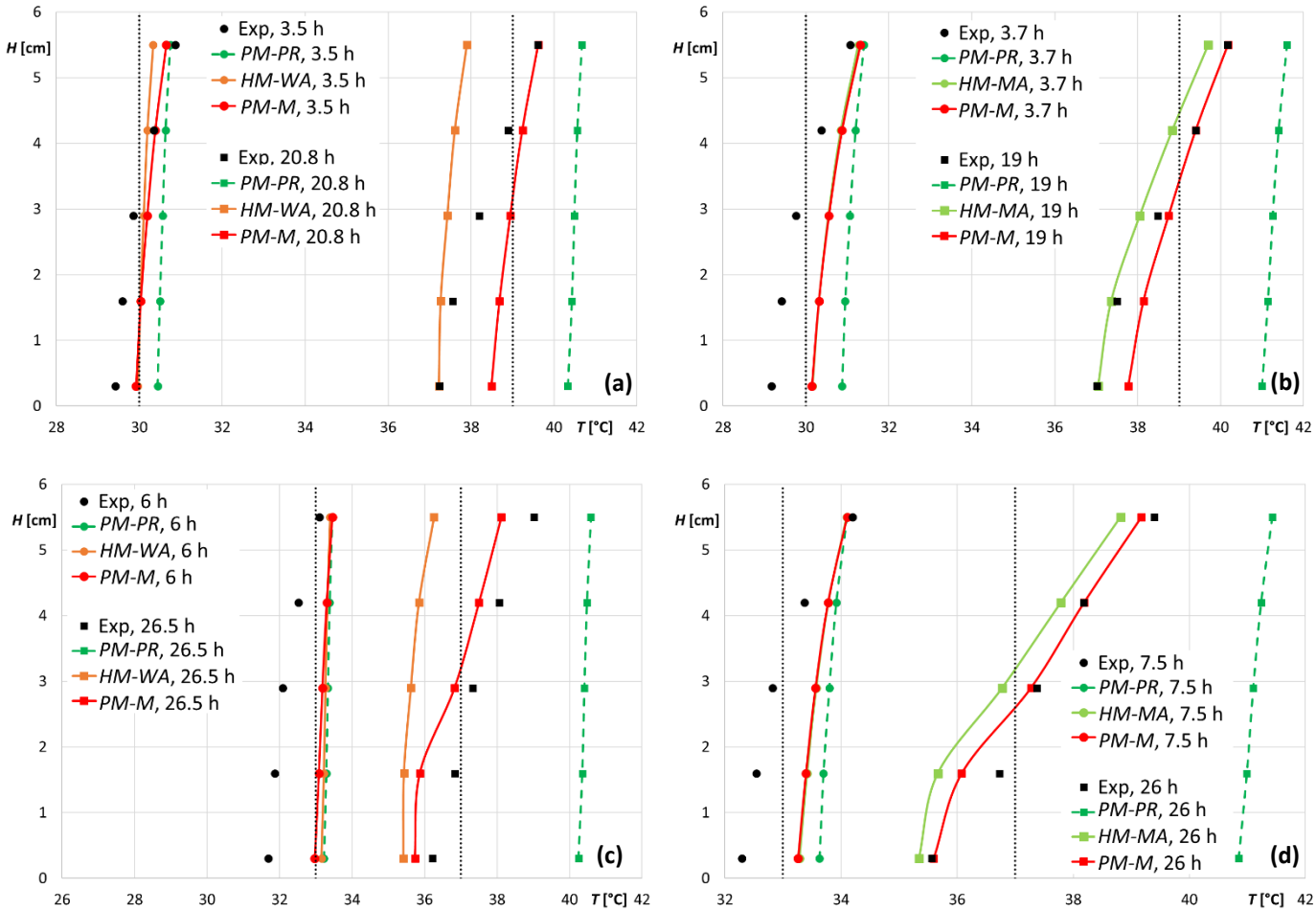

Fig. 11 Constant-time curves as functions of height (H) and temperature (T), recorded by the thermocouples and evaluated numerically with selected literature models and *Modified Porous-Medium* model, RT35 with copper (a), RT35 with aluminum (b), RT35HC with copper (c), RT35HC with aluminum (d).

5. Conclusions

In this paper a critical overview of the methods proposed in the literature for the estimation of the effective thermal properties of composite media in which PCMs are loaded with open-cell metal foams (copper and aluminum) is shown. The numerical results obtained by adopting the most popular correlations proposed for the estimation of the effective properties of metal-foam loaded PCMs have been compared with a series of specific experimental data, obtained by testing commercial paraffins

(RT35 and RT35HC) loaded with copper and aluminum foams having similar porosity (95-96%) and different pore density (10 PPI for aluminum and 20 PPI for copper).

It has been demonstrated that many of the available correlations for the estimation of the effective thermal properties of metal-foam loaded PCMs are not able to predict correctly the experimental results obtained by testing different combinations of PCMs and metal foams.

In particular, the available correlations associate to the metal-foam loaded PCM very different values of the effective thermal conductivity (in this case from 0.2 to 19.7 W/(m·K)), which generate strong differences in terms of temperature field obtained numerically. In addition, there is not a correlation available in the literature which gives accurate results for all the PCM-metal foams combinations tested in this work.

In order to solve this problem, in this work a new method for the calculation of the effective thermal conductivity of the composite PCM-metal foam medium is suggested. The method, easily implementable in COMSOL Multiphysics, is based on a simplified version of Bhattacharya's correlation deducted for high porosity metal foams.

It has been demonstrated how, following this method, the obtained numerical predictions are in good agreement with the experimental results obtained by considering all the PCM-metal foam combinations tested in this work.

The quality of the new method is due to the combination of an accurate estimation of the effective thermal conductivity value (Bhattacharya *et al*. correlation [35] is a weighted mean between the values of conduction in parallel and in series) and a precise numerical approach (the *Porous-medium* model, which considers a porous metal solid filled with a fluid, where only the latter changes phase).

Last but not least, it is well known that, in presence of heat transfer, two-energy equations models in which solid and PCM are not considered in local thermal equilibrium are generally more accurate than models based on local thermal equilibrium (one-energy equation), like the ones described in this paper. However, as demonstrated by the results shown in this paper, the low accuracy of the models based on the local thermal equilibrium assumption can be strongly improved if an accurate correlation and a precise numerical approach (the *Porous-medium* one) are employed, with the added advantage of the implementation of a fast and simpler numerical model.

Acknowledgements

This research has been granted by the Emilia-Romagna Regional development fund POR-FESR 2014-2020 Program under the CLIWAX project.

References

[1] European Union, Directive 2018/844 of the European Parliament and of the Council of 30 May 2018 amending Directive 2010/31/EU on the Energy Performance of Buildings and Directive 2012/27/EU on Energy Efficiency, Brussels, Belgium, 2018.

[2] R. Zeinelabdein, S. Omer, G. Gan, Critical review of latent heat storage systems for free cooling in buildings, Renewable and Sustainable Energy Reviews 82 (2018) 2843-2868.

[3] Y. Li, S. Liu, Y. Zhang, Experimental study of the heat transfer performance of PCMs within metal finned containers, Progress in Sustainable Energy Technologies 2 (2014) 669-684.

[4] M. Fadl, P.C. Eames, An experimental investigation of the heat transfer and energy storage characteristics of a compact latent heat thermal energy storage system for domestic hot water applications, Energy 188 (2019) 116083.

[5] H.J. Xu, C.Y. Zhao, Analytical considerations on optimization of cascaded heat transfer process for thermal storage system with principles of thermodynamics, Renewable Energy 132 (2019) 826-845.

[6] C. Pagkalos, G. Dogkas, M.K. Koukou, J. Konstantaras, K. Lymperis, M.G. Vrachopoulos, Evaluation of water and paraffin PCM as storage media for use in thermal energy storage applications: A numerical approach, International Journal of Thermofluids 1-2 (2020) 100006.

[7] M. Esapour, A. Hamzehnezhad, A.A.R. Darzi, M. Jourabian, Melting and solidification of PCM embedded in porous metal foam in horizontal multi-tube heat storage system, Energy conversion and management 171 (2018) 398-410.

[8] S. Rostami, M. Afrand, A. Shahsavar, M. Sheikholeslami, R. Kalbasi, S. Aghakhani, M. Safdari Shadloo, H.F. Oztop, A review of melting and freezing processes of PCM/nano-PCM and their application in energy storage, Energy 211 (2020) 118698.

[9] M.M. El Idi, M. Karkri, Heating and cooling conditions effects on the kinetic of phase change of PCM embedded in metal foam, Case Studies in Thermal Engineering 21 (2020) 100716.

[10] P.H. Biwole, D. Groulx, F. Souayfane, T. Chiu, Influence of fin size and distribution on solid-liquid phase change in a rectangular enclosure, International Journal of Thermal Sciences 124 (2018) 433-446.

[11] A. Al-Abidi, S. Mat, K. Sopian, M. Sulaiman, A. T. Mohammad, Numerical study of PCM solidification in a triplex tube heat exchanger with internal and external fins, International Journal of Heat and Mass Transfer 61 (2013) 684-695.

[12] A. Ji, Z. Qin, Z. Low, S. Dubey, F.H. Choo, F. Duan, Non-uniform heat transfer suppression to enhance PCM melting by angled fins, Applied Thermal Engineering 129 (2018) 269-279.

[13] M. Arici, E. Tutuncu, M. Kan, H. Karabay, Melting of nanoparticle-enhanced paraffin wax in a rectangular enclosure with partially active walls, International Journal of Heat and Mass Transfer 104 (2017) 7-17.

[14] L. Colla, L. Fedele, S. Mancin, L. Danza, O. Manca, Nano-PCMs for enhanced energy storage and passive cooling applications, Applied Thermal Engineering 110 (2017) 584-589.

[15] J. Krishna, P. Kishore, A.B. Solomon, Heat pipe with nano enhanced-PCM for electronic cooling application, Experimental Thermal and Fluid Science 81 (2017) 84-92.

[16] A.V. Arasu, A.S. Mujumdar, Numerical study on melting of paraffin wax with Al2O3 in a square enclosure, International Communications in Heat and Mass Transfer 39 (2012) 8-16.

[17] L.F. Cabeza, H. Mehling, S. Hiebler, F. Ziegler, Heat transfer enhancement in water when used as PCM in thermal energy storage, Applied Thermal Engineering 22 (2002) 1141-1151.

[18] J. Cheng, G. Chen, S. Li, F. Hou, High-thermal-conductivity phase-change composites prepared by in situ synthesis of graphite Nanoplatelets/Cu networks for effective thermal management, Journal of Energy Storage 41 (2021) 102952.

[19] F. Samimi, A. Babapoor, M. Azizi, G. Karimi, Thermal management analysis of a Li-ion battery cell using phase change material loaded with carbon fibers, Energy 96 (2016) 355-371.

[20] G. Righetti, L. Doretti, C. Zilio, G.A. Longo, S. Mancin, Experimental investigation of phase change of medium/high temperature paraffin wax embedded in 3D periodic structure, International Journal of Thermofluids 5 (2020) 100035.

[21] G. Righetti, G. Savio, R. Meneghello, L. Doretti, S. Mancin, Experimental study of phase change material (PCM) embedded in 3D periodic structures realized via additive manufacturing, International Journal of Thermal Sciences 153 (2020) 106376.

[22] Z.A. Qureshi, S.A.B. Al-Omari, E. Elnajjar, O. Al-Ketan, R.A. Al-Rub, Using Triply Periodic Minimal Surfaces (TPMS)-based Metal Foams Structures as Skeleton for Metal-Foam-PCM Composites for Thermal Energy Storage and Energy Management Applications, International Communications in Heat and Mass Transfer 124 (2021) 105265.

[23] R.D.C. Oliveski, F. Becker, L.A.O. Rocha, C. Biserni, G.E.S. Eberhardt, Design of fin structures for phase change material (PCM) melting process in rectangular cavities, Journal of Energy Storage 35 (2021) 102337.

[24] V. Shatikian, G. Ziskind, R. Letan, Numerical investigation of a PCM-based heat sink with internal fins, International Journal of Heat and Mass Transfer 48 (2005) 3689-3706.

[25] M. Sheikholeslami, R. Haq, A. Shafee, Z. Li, Heat transfer behavior of nanoparticle enhanced PCM solidification through an enclosure with V shaped fins, International Journal of Heat and Mass Transfer 130 (2019) 1322-1342.

[26] R. Kalbasi, M. Afrand, J. Alsarraf, M-D. Tran, Studies on optimum fins number in PCM-based heat sinks, Energy 171 (2019) 1088-1099.

[27] B. Kok, Examining effects of special heat transfer fins designed for the melting process of PCM and Nano-PCM, Applied Thermal Engineering 170 (2020) 114989.

[28] T.U. Rehman, H.M. Ali, M.M. Janjua, U. Sajjad, W.-M. Yan, A critical review on heat transfer augmentation of phase change materials embedded with porous materials/foams, International Journal of Heat and Mass Transfer 135 (2019) 649-673.

[29] A.P. Zhang, Z. Meng, H. Zhu, Y. Wang, S. Peng, Melting heat transfer characteristics of a composite phase change material fabricated by paraffin and metal foam, Applied Energy 185 (2017) 1971-1983.

[30] A. Alhusseny, N. Al-Zurfi, A. Nasser, A. Al-Fatlawi, M. Aljanabi, Impact of using a PCM-metal foam composite on charging/discharging process of bundled-tube LHTES units, International Journal of Heat and Mass Transfer 150 (2020) 119320.

[31] M.H.S. Abandani, D.D. Ganji, Melting effect in triplex-tube thermal energy storage system using multiple PCMs-porous metal foam combination, Journal of Energy Storage 43 (2021) 103154.

[32] C. Yu, Q. Peng, X. Liu, P. Cao, F. Yao, Role of metal foam on ice storage performance for a cold thermal energy storage (CTES) system, Journal of Energy Storage 28 (2020) 101201.

[33] H.A. Ahmadi, N. Variji, A. Kaabinejadian, M. Moghimi, M. Siavashi, Optimal design and sensitivity analysis of energy storage for concentrated solar power plants using phase change material by gradient metal foams, Journal of Energy Storage 35 (2021) 102233.

[34] X. Chen, X. Li, X. Xia, C. Sun, R. Liu, Thermal Performance of a PCM-Based Thermal Energy Storage with Metal Foam Enhancement, Energies 12 (2019) 3275.

[35] A. Bhattacharya, V.V. Calmidi, R.L. Mahajan, Thermophysical properties of high porosity metal foams, International Journal of Heat and Mass Transfer 45 (2002) 1017-1031.

[36] G. Righetti, R. Lazzarin, M. Noro, S. Mancin, Phase change materials embedded in porous matrices for hybrid thermal energy storages: Experimental results and modeling, International Journal of Refrigeration 106 (2019) 266-277.

[37] T.U. Rehman, H.M. Ali, Experimental study on the thermal behavior of RT-35HC paraffin within copper and Iron-Nickel open cell foams: energy storage for thermal management of electronics, International Journal of Heat and Mass Transfer 146 (2020) 118852.

[38] H. Mhiri, A. Jemni, H. Sammouda, Numerical and Experimental Investigations of Melting Process of Composite Material (nanoPCM/carbon Foam) Used for Thermal Energy Storage, Journal of Energy Storage 29 (2020) 101167.

[39] P. Tittelein, S. Gibout, E. Franquet, K. Johannes, L. Zalewski, F. Kuznik, J.P. Dumas, S. Lassue, J.P. Bédécarrats, D. David, Simulation of the thermal and energy behaviour of a composite material containing encapsulated-PCM: Influence of the thermodynamical modelling, Applied Energy 140 (2015) 269-274.

[40] S.N. AL-Saadi, Z. Zhai, Modeling phase change materials embedded in building enclosure: A review, Renewable and Sustainable Energy Reviews 21 (2013) 659–673.

[41] M. Iten, S. Liu, A. Shukla, Experimental validation of an air-PCM storage unit comparing the effective heat capacity and enthalpy methods through CFD simulations, Energy 155 (2018) 495-503.

[42] Y. Khattari, T. El Rhafiki, N. Choab, T. Kousksou, M. Alaphilippe, Y. Zeraouli, Apparent heat capacity method to investigate heat transfer in a composite phase change material, Journal of Energy Storage 28 (2020) 101239.

[43] S. Lorente, A. Bejan, J.L. Niu, Phase change heat storage in an enclosure with vertical pipe in the center, International Journal of Heat and Mass Transfer 72 (2014) 329-335.

[44] A. Caggiano, C. Mankel, E. Koenders, Reviewing Theoretical and Numerical Models for PCM-embedded Cementitious Composites, Buildings 9 (2019) 3.

[45] A.S. Fleischer, Thermal Energy Storage Using Phase Change Materials - Fundamentals and Applications, Springer, Minneapolis, 2015, pp. 80-94.

[46] H.J. Xu, Thermal transport in microchannels partially filled with micro-porous media involving flow inertia, flow/thermal slips, thermal non-equilibrium and thermal asymmetry, International Communications in Heat and Mass Transfer 110 (2020) 104404.

[47] D.A. Nield, A. Bejan, Convection in porous media. In: A. Bejan, Convection heat transfer, John Wiley & Sons, Hoboken, 2013, pp. 537-605.

[48] O. Mesalhy, K. Lafdi, A. Elgafy, K. Bowman, Numerical study for enhancing the thermal conductivity of phase change material (PCM) storage using high thermal conductivity porous matrix, Energy Conversion and Management 46 (2005) 847–867.

[49] Z. Wang, Z. Zhang, L. Jia, L. Yang, Paraffin and paraffin/aluminum foam composite phase change material heat storage experimental study based on thermal management of Li-ion battery, Applied Thermal Engineering 78 (2015) 428-436.

[50] COMSOL Multiphysics, Heat Transfer Module User's Guide, https://doc.comsol.com/ (last accessed on 13 January 2022).

[51] A. Chamkha, A. Veismoradi, M. Ghalambaz, P. Talebizadehsardari, Phase change heat transfer in an L-shape heatsink occupied with paraffin-copper metal foam, Applied Thermal Engineering 177 (2020) 115493.

[52] C. Amaral, R. Vicente, V.M. Ferreira, T. Silva, Polyurethane foams with microencapsulated phase change material: Comparative analysis of thermal conductivity characterization approaches, Energy and Buildings 153 (2017) 392–402.

[53] P. Ranut, On the effective thermal conductivity of aluminum metal foams: Review and improvement of the available empirical and analytical models, Applied Thermal Engineering 101 (2016) 496–524.

[54] H.J. Xu, Z.B. Xing, F.Q. Wang, Z.M. Cheng, Review on heat conduction, heat convection, thermal radiation and phase change heat transfer of nanofluids in porous media: Fundamentals and applications, Chemical Engineering Science 195 (2019) 462-483.

[55] J.C. Maxwell Garnett, Colours in metal glasses and in metallic films, Philosophical Transactions of the Royal Society of London A 203 (1904) 385–420.

[56] J.C. Maxwell Garnett, Colours in metal glasses, in metallic films, and in metallic solutions II, Philosophical Transactions of the Royal Society of London 205 (1906) 237–288.

[57] R. Lemlich, A Theory for the Limiting Conductivity of Polyhedral Foam at Low Density, Journal of Colloid and Interface Science 64 (1978) 107-110.

[58] J.A. Weaver, R. Viskanta, Freezing of Liquid-Saturated Porous Media, ASME Journal of Heat Transfer 108 (1986) 654-659.

[59] H. Inaba, P. Tu, Evaluation of thermophysical characteristics on shape-stabilized paraffin as a solid-liquid phase change material, Heat and Mass Transfer 32 (1997) 307–312.

[60] X. Xiao, P. Zhang, M. Li, Effective thermal conductivity of open-cell metal foams impregnated with pure paraffin for latent heat storage, International Journal of Thermal Sciences 81 (2014) 94-105.

[61] W.Q. Xu, X.G. Yuan, Z. Li, Study on effective thermal conductivity of metal foam matrix composite phase change materials, Journal of Functional Materials 40 (2009) 1329-1337 (in Chinese).

[62] S.T. Hong, D.R. Herling, Effects of Surface Area Density of Aluminum Foams on Thermal Conductivity of Aluminum Foam-Phase Change Material Composites, Advanced Engineering Materials 9 (2007) 554-557.

[63] H.L. Zhang, J. Baeyens, J. Degrève, G. Cáceres, R. Segal, F. Pitié, Latent heat storage with tubular-encapsulated phase change materials (PCMs), Energy 76 (2014) 66-72.

[64] M.O.R. Siddiqui, D. Sun, Computational analysis of effective thermal conductivity of microencapsulated phase change material coated composite fabrics, Journal of Composite Materials 49 (2015) 2337–2348.

[65] P. Di Giorgio, M. Iasiello, A. Viglione, M. Mameli, S. Filippeschi, P. Di Marco, A. Andreozzi, N. Bianco, Numerical Analysis of a Paraffin/Metal Foam Composite for Thermal Storage, Journal of Physics: Conference Series 796 (2017) 012032.

[66] H. Xu, Y. Wang, X. Han, Analytical considerations of thermal storage and interface evolution of a PCM with/without porous media, International Journal of Numerical Methods for Heat & Fluid Flow 30 (2020) 373-400.

[67] C.Q. Wu, H.J. Xu, C.Y. Zhao, A new fractal model on fluid flow/heat/mass transport in complex porous structures, International Journal of Heat and Mass Transfer 162 (2020) 120292.

[68] N. Bianco, S. Busiello, M. Iasiello, G.M. Mauro, Finned heat sinks with phase change materials and metal foams: Pareto optimization to address cost and operation time, Applied Thermal Engineering 197 (2021) 117436.

[69] K. Venkateshwar, S.H. Tasnim, H. Simha, S. Mahmud, Empirical correlations to quantify the effect of metal foam on solidification process in constant thermal capacity and constant volume systems, Journal of Energy Storage 30 (2020) 101482.

[70] S. Cancellara, M. Greppi, M. Dongellini, G. Fabbri, C. Biserni, G.L. Morini, Experimental Investigation on the Pressure Drop of Air Flows Through Aluminum and Nickel-Chromium Metallic Foams for HVAC Applications, Energies 13 (2020) 172.

[71] R.J. Moffat, Describing the Uncertainties in Experimental Results, Experimental Thermal and Fluid Science 1 (1988) 3-17.

[72] T.L. Bergman, A.S. Lavine, F.P. Incropera, D.P. DeWitt, Fundamentals of heat and mass transfer, John Wiley & Sons, Hoboken, 2011, pp. 559-618.